Nonlinear SISO System Identification Applied to the Series System Power-Driver, DC-Motor and Propeller

José Fort, José Gaspar
Instituto Superior Técnico / UTL, Lisbon, Portugal
joforrui@gmail.com, jag@isr.ist.utl.pt

Abstract

In this report is proposed a least squares methodology to estimate the parameters of a non-linear system composed by one Power Driver, one DC Motor and one Propeller. The input of the system is the reference power and the output is the rotation speed of the two blades propeller.

Two parametrizations are considered. The parametrizations differ whether the main non linear effect is associated to (i) the propeller, or (ii) the power driver. In addition, the estimation process is assessed based in a sensitivity analysis. This analysis is performed using a numerical procedure where Gaussian noise is added to the response of a simulated system, and then the system parameters are recomputed based in the noisy data.

Data acquired from a real system is used to test the parameters estimation methodology. Then, the estimation results are used to assess whether the real system has a non-linear effect more, or lesser, severe in the power driving or the propeller. The sensitive analysis is performed on the best fitting model.

I. Introduction

The motivation for this work comes from an EEC course on Real Time Distributed Control Systems lectured by Professor Carlos Silvestre [5]. This course involves, among other tasks, regulating the height of a levitating ball enclosed in a vertical tube. The ball is actuated by a propeller coupled to a DC motor. The reference values are sent to the motor by a dedicated microcontroller, which also acquires ball-height measurements and interfaces to a dedicated PC through a CAN bus.

Power driver, DC motor and propeller (PMP), form the actuation component of the complete setup and is the subsystem to be identified in this work. The propeller introduces by itself a nonlinear (quadratic) relationship between the motor spinning speed and the propelling force. The power driver is composed by one single MOSFET transistor, working in saturation and pulsed by a PWM signal, hence adding another nonlinear component to the system. The purpose of our work is to identify the PMP as a continuous system, using an approximate model. We include the non-linear terms in the PMP model in order to obtain a more accurate real system identification.

Given that the main motivation of this work comes from a didactic setup, and the work has the purpose of continuing to serve didactic purposes, we seek to propose and validate simple identification methodologies. As noted in work [1], entitled *Nonlinear system identification is simple*, knowing the state of a continuous system and its derivatives as functions of the control and output variables, is equivalent to know the system itself. Commonly, one has sensors giving observations of the state but not of its time derivatives. In order to identify the system, one can than follow a system discretization approach [2] or, more recently, try to estimate directly the derivatives using filtering kernels [1], [6]. We follow the later approach, by considering simple, non-causal, first order, difference kernels to estimate the state derivatives.

More in detail, the thesis encompasses the proposal of a model for the PMP system, the identification of the parameters of the model given real data, and a sensibility analysis of the identification methodology.

We start by modeling each of the three subsystems composing the PMP system using physics. Then the partial models are combined. The resulting model has the form of a non-linear differential equation, having as input the motor reference voltage and as state, and output, the rotation speed of the propeller. The partial models introduce non linear components into the complete system model.

Having obtained the non linear model, we introduce one methodology to estimate the parameters of the model. The methodology is based in least squares, comparing real-system responses with model-based responses. Real system data encompasses input, state and derivative state signals. This information is obtained with a data acquisition card and signal preprocessing as, e.g., a Schmitt-Trigger to attenuate noise. The data acquired allows fitting various models, more precisely various numbers of parameters, indicating different combinations of the various non-linearities, and therefore assessing the relative importance of the non-linearities.

Finally, a sensibility analysis, based on noise added to the sensor and re-estimation of parameters, considering the best fit model, allows assessing the validity of the methodology.

The report follows the following structure: Section 2 introduces the system studied in this master thesis. We divide the complete system into three subsystems and detail their non linear components. This chapter ends with the problem formulation on non linear systems identification. Section 3

presents the identification methodology based in the estimation of model parameters. Non-linear terms are included to represent accurately the real system in a least squares sense. Section 4 details the experiments conducted in this dissertation. This chapter is composed by two main sections. The first one identifies the PMP real model. The second section assesses the effect of sensor noise into the identification of the system. Section 5 summarizes the results obtained along the thesis, indicates alternative ideas for non-linear system identification and presents suggestions for future work.

II. Setup Power-Motor-Propeller

In this section is detailed the nonlinear system considered in this thesis. The system is composed of three main subsystems connected in series: Power-Driver, DC-Motor and Propeller. In the following the acronym PMP is used to indicate the complete system. Figure 1 shows the whole system.

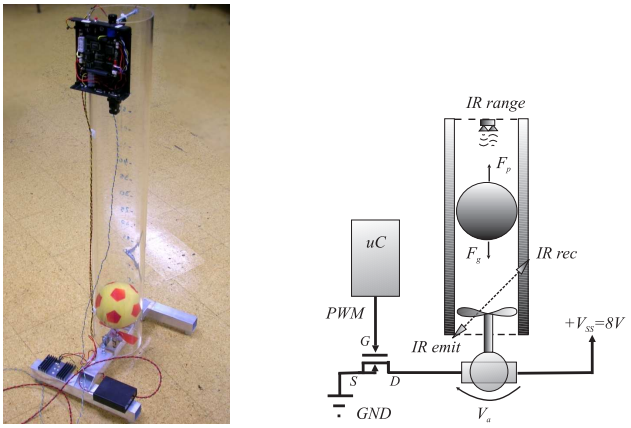

Fig. 1. Photograph and diagram of the levitating ball setup.

One central objective of this thesis is the identification of the PMP model. We follow a parametric model based approach. We start by introducing the parametric model.

The aim of PMP system is to keep one ball inside a tube in a wanted height. To get the ball flying we use the propeller driven by a DC-Motor through a shaft. The DC-Motor provides the torque to make the propeller spin and the latter keeps the ball in the air. The DC-Motor is driven by the current provided by the switched ON/OFF MOSFET. The MOSFET amplifies the power of PWM signal provided by a micro controller.

As figure 1 shows, we use one infrared sensor emitter/receiver interrupted by the blades of the propeller to get the output speed measurements. This sensor counts the spin times of the blades allowing therefore to obtain the propeller speed.

In summary, the PMP system is a SISO system: has one input, the PWM signal, and one output, the rotating speed of the propeller.

As a general non-linear dynamic system the PMP system can be described as:

$$\begin{cases} \dot{x}(t) = f\left(x(t), u(t); \theta\right) \\ y(t) = g\left(x(t), u(t); \theta\right) \end{cases} \tag{1}$$

where x is the system state (in our case the speed of the blades), u is the control input (v_s, the signal that comes from the micro controller), y are the measurements that comes from the IR sensors and f, g denoting nonlinear system and measurements functions. θ represents the parameters of the system. These are the parameters which we are interested to identify.

In this work the system can be represented (or approximated) by dynamic models whose derivatives are weighted sums of powers of the state and of the input, i.e. an approach similar to the polynomial black-box system representation as suggested by [2]:

$$\dot{x} = -\sum_{i=1}^{N} a_i x^i + \sum_{j=0}^{M} b_j u^j \tag{2}$$

where N is the maximum exponent of the state variable and M the maximum exponent of the input variable. We assume that the measurements allow to estimate directly an uni dimensional state $g(x, u) = x$ and that the equation can be approximated by a polynomial model. In the following we show that out PMP can be approximated by the model (2).

A. Power Driver

We begin by detailing the power-driver subsystem. One MOSFET provides the current that supplies the DC-Motor and likewise speed to the fan blades. The MOSFET is used to switch ON/OFF the power supply while consuming low currents.

The transistor is commanded through the gate to source voltage v_{GS}, by a pulse-width-modulated (PWM) signal generated by a micro controller ($0 - 5$ Volt signal).

When $v_{GS} = 0$ V, the transistor is in the cut-off mode, and v_{DS} has its highest value. When $v_{GS} = 5$ V, the transistor is turned ON, and the channel becomes close to a very low resistance state (resistance typically one order of magnitude lower than the already typically small resistance of the motor). The transition from cut-off to the ohmic mode, implies transients where v_{DS} is still large and thus the MOSFET has a saturation behavior during the transient.

Assuming that the counter electromotive force is approximately zero, $v_{cemf} \approx 0$ and $L_a \approx 0$, one has that $i_a = (V_{SS} - v_{DS})/R_a$. Considering transient saturation and ohmic modes, the current of the MOSFET, i_a has linear, mixed with quadratic, relationships with the gate-to-source, v_{GS} and drain-to-source, v_{DS} voltages as it shows the plot in figure 2 [3].

In the ohmic zone the quadratic relationship between the current of the MOSFET and the gate-to-source and drain-to-source voltage are modeled by:

$$i_D = K v_{DS}^2 \tag{3}$$

where $v_{DS} = v_{GS} - v_{GSth}$, v_{GSth} is the gate-to-source threshold voltage and K is a constant value that depends of the transistor geometry. The right side of the figure 2 shows the quadratic behavior of the MOSFET and its linear approximation.

The transistor in conjunction with the motor, Eq. (15), will exhibit rational relationships of i_a with v_{GS} and/or v_{GS}^2, depending on the operating mode.

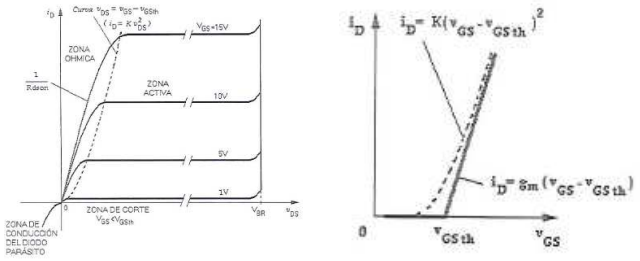

Fig. 2. MOSFET type n (Left). MOSFET transfer function $i_D(v_{GS})$ and working regions (right). Figure extracted from [3].

The PWM signal sets the voltage to the DC-Motor within the range 0%-100% of the main power supply by commanding the MOSFET.

B. DC-Motor

In this subsection we introduce the DC-Motor equations for our PMP system. Figures 3 illustrates the two main subsystems, (i) electrical and (ii) mechanical.

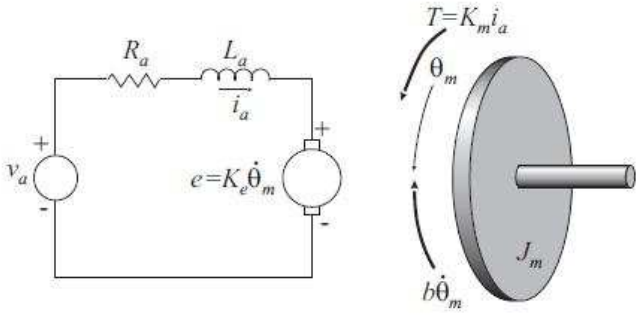

Fig. 3. Parameters of a DC motor. Figure extracted from [4].

The equation that models the electrical subsystem using the Kirchhoff voltage law is:

$$V_a - I_a(t)R_a - L_a\dot{I_a}(t) - V_{cemf} = 0 \tag{4}$$

where V_{cemf} is the counter electromotive force.

The mechanical equation is based in Newton's second law for rotation:

$$J\ddot{\theta_m} = T_m(t) - b\dot{\theta} \tag{5}$$

where J is the inertia of the DC-Motor, $T_m(t)$ is the DC-Motor torque, $\ddot{\theta}_m$ is the angular speed of the DC-Motor and b is the friction coefficient of the DC-Motor. We assume the friction coefficient of the DC-Motor and the angular speed of the DC-Motor is the same that the angular speed of the blades $\ddot{\theta} = \ddot{\theta}_m$.

The electric and mechanical equations are linked by the torque built by the current. The mechanical power is equal to torque times the rotation speed, $P = T_m w$. The electric power is computed as $V_a I_a = I_a^2 R_a + E_b I_a$. Considering that $I_a^2 R_a$ are losses (heat dissipated) in the resistive part of the circuit, one has that the power delivered to the mechanical component is

$$P = eI_a = T\dot{\theta_m} \tag{6}$$

where

$$e = V_{cemf} = \frac{\frac{(P\phi Z)}{AN}}{60} = \frac{K_b N}{60} \quad \text{and} \quad \dot{\theta_m} = \frac{(2\pi N)}{60}. \tag{7}$$

where N denotes the rotation speed in [rpm].

Then, we have

$$T(t) = \frac{K_b}{2\pi} I_a(t) = K_m I_a(t) \tag{8}$$

having just obtained a relationship of torque with current.

Finally, the fan works due to DC motor [1] and owing to the second law of Newton, the difference on the pressure between the providing pressure of the fan and the pressure above it (atmospheric) the ball could levitate higher or lower.

C. Propeller

The propeller is the last subsystem of the PMP model. It is the responsible to keep the ball in the air at a desired height. Our propeller has two blades and is connected by an axis to the DC-Motor that provides torque to move it. The blades are modeled by:

$$T_h(t) = -K_{h_1}\dot{\theta}(t) - K_{h_2}\dot{\theta}^2(t) \tag{9}$$

where

- $T_h(t)$ is the blades torque
- K_{h1} is the friction coefficient of the blades proportional to the angular speed $[N.m.rad^{-}1.s]$
- K_{h2} is the friction coefficient of the blades proportional to the square angular speed $[N.m.rad^{-2}.s^2]$
- $\dot{\theta}(t)$ is the angular speed of the blades.

Equation (9) shows the torque opposite to the torque moving the blades.

As explained before, we measure the rotation speed of the blades using one infrared sensor (emitter/receiver) to get the output speed measurements counting the spin times of the blades.

The last subsystem is the ball-tube system where the ball is located as it could be seen in figure 4. To ease (or not make it unnecessarily hard), the ball and fan will be considered like discs.

Figure 4 shows the difference between the real process and our mathematical model. Pressures P_1 and P_4 are in contact with the air so are the same as the atmospheric pressure, P_2 is the pressure from the fan and P_3 is the force that makes go up or down the ball. Then, we have to find the expressions that give us the pressure below the ball and the force balance in the ball. The equation of the force balance in the ball is based in Newton's second law:

$$m\ddot{z}(t) = A(P_3 - P_4) - mg \tag{10}$$

[1]The DC-Motor used is the Graupner 500 sp which has a nominal voltage : 8.4V, No-load rpm = $32000min^{-1}$. This motor is typically used for model flight, then enough for our purpose.

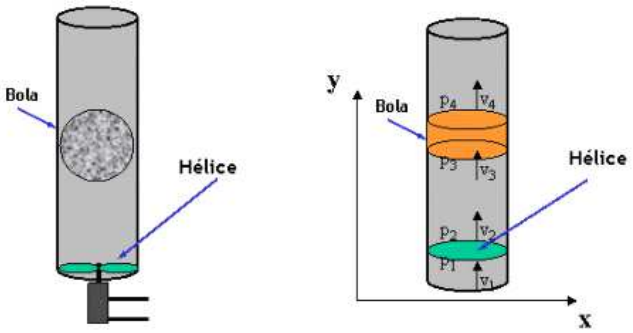

Fig. 4. Real system propels a ball (left) while the approximate model is based in a disc (right). Figure extracted from [5].

where m is the mass of the ball, $z(t)$ is the vertical position in the tube, A is the area of the ball (same as the area of an orthogonal section of the tube), and g is the gravitational acceleration.

For the pressure below the ball, we use the Bernoulli's law. This law is valid for all the fluids, including air, which is the case of our setup:

$$P_i + \frac{1}{2}\rho v_i^2 + gz_i = P_{i-1} + \frac{1}{2}\rho v_{i-1}^2 + gz_{i-1} \qquad (11)$$

In the cases $i = 3$ and $i = 2$ we can do many simplifications like assuming that air is an ideal fluid and therefore the density and velocity are the same in both sides owing to the short length of the tube. We can assume also that the ball is represented by a thin disk, i.e. $Z_3 = Z_2$. After the simplifications, one obtains $P_3 = P_2$. The next step is to find the value P_2. From the assumption that the ball can be represented as a disc, we obtain P_2 by considering that the propeller produces pressure as a force divided the cylinder area:

$$P_2 = P_1 + \frac{F(t)}{A} \qquad (12)$$

The equation of the force generated by the fan is:

$$F(t) = \frac{1}{4}\rho n_p c(\Omega(t)R)^2 R a_o \theta_o \qquad (13)$$

where n_p is the number of blades in the fan, c is the width of the blades, Ω is the angular velocity, R is the fan radius, θ_o is the blade incident angle, and a_o is the aerodynamics constant.

Noting that Ω is the variable of interest, a much simpler model can be proposed:

$$F(t) = K_h(t)\Omega^2(t) \qquad (14)$$

where K_h is a constant to be determined experimentally.

D. Complete PMP Model

Figure 5 shows that the PMP model is composed by the Propeller, DC-Motor and the input provided by the Power Driver. The objective of this section is to summarize the equations that connect all the subsystems together to form just one.

The propeller introduces by itself a nonlinear (quadratic) relationship between the motor spinning speed and the propelling force. The power driver is composed by one single

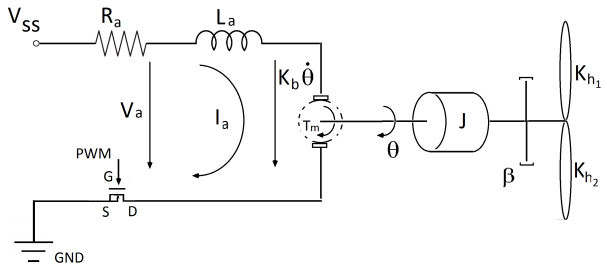

Fig. 5. Motor and Propeller Model. Figure extracted from [5].

MOSFET transistor, working in saturation and pulsed by a PWM signal, hence adding another nonlinear component to the system. The purpose of our work is to identify the PMP as a continuous system, using an approximate model.

Watching the figure 5 and applying the Kirchhoff voltage law we have the following equation which relates the power driver with DC-Motor.

$$V_{SS} = R_a I_a + L_a \frac{d}{dt} i_a + v_{cemf} + v_{DS} \qquad (15)$$

where V_{SS} is the power supply, V_{cemf} is counter electromotive force and v_{DS} is the voltage coming from the MOSFET.

Equations (6) and (7) allow connecting the axis with the DC-Motor in function with the counter electromotive force as follows:

$$T_m(t) = K_b/2\pi I_a(t) = K_m I_a(t)\ . \qquad (16)$$

The first non linearity that appears in our system is located in the Power Driver, more precisely on the MOSFET. The equation (3) shows the non linearity behavior during the transient ohmic mode to the saturation region.

We use a simplification of these rational relationships. In order to characterize the effect of the PWM average value and, more precisely, its programming value v_{ref}, used in the micro controller software[2], to the torque generated by the motor, T_m, which is proportional to the current, $T_m = K_m i_a$, we use the simplified model:

$$T_m = \beta_0 + \beta_1 v_{ref} + \beta_2 v_{ref}^2. \qquad (17)$$

The second non linearity appears on the dynamics between the DC-Motor and fan, more precisely owing to the friction blades with the air when they try to move is modeled by the equation (9).

Now, we just need the last balance to connect the blades to our system, Taking equation (17) we have:

$$J\ddot{\theta}(t) = T_m(t) - T_h(t) \qquad (18)$$

where T_m is the torque of the DC motor and T_h is the opposite torque of the blades. Then

$$J\ddot{\theta}(t) = T_m(t) - K_{h_1}\dot{\theta}(t) - K_{h_2}\dot{\theta}^2(t). \qquad (19)$$

[2]There is a linear relationship between the PWM programming values, v_{ref} ranging $0 \cdots 255$, and the average value of the PWM signal, $\int_t^{t+T} v_{GS}(t)dt/T$, ranging $0 \cdots 5$ V.

Equation 19 shows see that the only term giving momentum of inertia is torque. The damping coefficient of the fan reduces the momentum.

The PMP system links the DC-motor with the fan. The behavior and torque of the fan is described by the equations (18) and (19) respectively. Moreover, taking $w = \dot{\theta}$, $\alpha_1 = K_{h_1}$ and $\alpha_2 = K_{h_2}$ the new equation is:

$$T_h = \alpha_1 \omega + \alpha_2 \omega^2 \ . \tag{20}$$

Finally, putting together all the equations we have the following general model:

$$\dot{x} + a_1 x + a_2 x^2 = b_0 + b_1 u + b_2 u^2 \tag{21}$$

where $a_i = \alpha_i / J$, $u = v_{ref}$ and $b_i = \beta_i / J$, that is a particular case of the general polynomial equation (2) and will allow us to know the system itself as noted by [1] due to the derivative of the state system is a function of the control and output variables.

E. Problem Formulation

Non linear systems present some formulation problems and identification difficulties that linear systems do not. One of the aspects of non linear systems is that one cannot use the superposition principle and use it to obtain simple solutions.

In some cases nonlinear systems are approached as linear systems. The way to do it is by finding the work region and transforming this (limited) region into a linear system. It is important to compare and verify if the responses are similar to the approximation. If they are, then the identified model can be used to represent the real system. This approach can be used for relatively simple systems [3].

Fortunately, in our PMP setup the most significant effects of the non linear components can be observed easily with a sensor measuring the propeller rotation speed. In the next chapter will introduce two different identification methodologies based in equation (2). As previously mentioned, the didactic application of the system considered in this thesis indicate using simple models. We will take just the minimum parameters to describe the most significant non linearities.

III. Identification Methodology

In this section we use a least squares formulation to estimate the parameters of the model proposed for the series system, power-driver, DC-Motor and propeller (21).

A. Data Acquisition

Figure 6 shows the setup of the hardware and the pre-processing associated to data acquisition. Figure 6(a) shows the Power-Motor-Propeller system and the variables that model his behavior. The main variable to that model is rotation speed, ω and the infrared voltage V_{IR}.

[3]Counter examples include chaotic systems in which it is impossible to predict what will happen. For example, weather forecast models require using large numbers of variables due to covering large areas, while encompassing many complex interactions within the covered areas. As it is impossible having one sensor per variable per place of interest, weather forecast is still, nowadays, frequently imprecise.

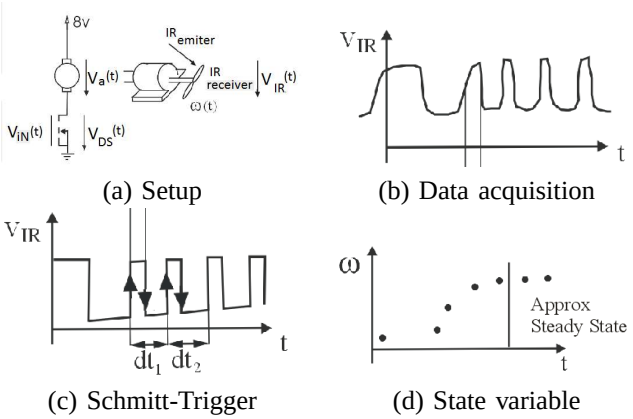

(a) Setup (b) Data acquisition

(c) Schmitt-Trigger (d) State variable

Fig. 6. Setup and data acquisition.

We use one infrared emitter and one receiver to count the number of times per second the two blades pass and cut the infrared light path. When the blade cut the light path, V_{IR} gets its maximum value. Then, to get the rotation speed is just needed to be counted the blades twice having in mind the time spent to do it. This is measured as time between two peeks on V_{IR}.

The real signal is not as clean as shown in the figure 6. It has associated sudden ON/OFF changes of the MOSFET which disturbs the ground voltage. The most effective solution to this problem is to introduce a Schmitt-Trigger. It is an active circuit which converts an analog input signal to a digital output signal. In the non-inverting configuration, when the input is higher than a certain chosen threshold, the output is high. When the input is below a different (lower) chosen threshold, the output is low, and when the input is between the two levels, the output retains its value.

IV. Model fit

In this section we consider the general model (2) and propose two least squares methodologies to identify the parameters of the model. The two methodologies are designed to handle the cases where one has steady state or dynamic system response measurements [4].

A. Steady state model fit

This model fit methodology is based in steady state measurements for various constant inputs. In other words we have u constant (reference) inputs, x constant measurements, and $\dot{x} = 0$. Taking this particular case into equation (2) one obtains:

$$-\sum_{i=1}^{N} a_i x^i + \sum_{j=0}^{M} b_j u^j = 0 \tag{22}$$

where a_i and b_i denote the parameters to estimate given a choice of orders N and M.

[4]Introductory, motivating, system identification formulations can be found in Appendix.

This problem is a particular case of (34). To find the optimal estimation of the steady state parameters, $\widehat{\theta_{SS}}$ can be formulated as:

$$\widehat{\theta_{SS}} = \arg_\theta \min \frac{1}{K} \sum_{k=1}^{K} [\ \phi(k)^T \theta\ ]^2 \quad s.t.\ \|\theta\| = 1 \tag{23}$$

where the matrix formulation of the variables is:

$$\phi(k) = [-x(k)\ -x(k)^2\ \cdots -x(k)^N\ 1\ u(k)\ u(k)^2\ \cdots\ u(k)^M]^T \tag{24}$$

and

$$\theta = [a_1\ a_2\ \cdots\ a_N\ b_0\ b_1\ b_2\ \cdots\ b_M]^T \tag{25}$$

Having measurements at K time samples, allows defining a $K \times (N+1+M)$ matrix $\phi_K = [\phi(1)\ \phi(2)\ \cdots\ \phi(K)]^T$ and estimating the system parameters from the right singular vector associated to the least singular value of ϕ.

In case one has the possibility of injecting steps to the system, and obtaining the step responses, $\{(t(k), x(k)) : k = 1 \cdots K\}$, one can promote the steady-state identification to a dynamic identification, by scaling $\widehat{\theta_{SS}}$. Let $\hat{x}(k)_{|u_\infty, \alpha\widehat{\theta_{SS}}}$ denote a simulated step response, at time t_k, to a step input with the steady state value u_∞, considering the scaled parameters $\alpha\widehat{\theta_{SS}}$. Then one can write another (nonlinear) least squares problem to find the scaling factor α:

$$\alpha^* = \arg \alpha \min \sum_{k=1}^{K} \left| x(k) - \hat{x}(k)_{|u_\infty, \alpha\widehat{\theta_{SS}}} \right|^2. \tag{26}$$

This problem can be solved having one single sample $(t(k), x(k))$, but the accuracy of the solution benefits of using as many as possible data samples. This nonlinear optimization problem requires simulation and a non trivial optimization routine as the Matlab's `fminsearch`. In the next section, we see that in case one has derivative estimates, then the problem is much simplified.

B. Dynamic model fit

When one has dynamic responses to generic (known) inputs, not necessarily just the step responses, and has a method to observe or estimate the derivatives, then it is possible to estimate directly the steady-state system parameters and its global scaling [1], [6].

In the following we consider a very simple, non-causal, first order, difference kernel, for low noise signals. We consider the derivative approximation:

$$\hat{\dot{x}}(k) = \frac{x(k+1) - x(k-1)}{t(k+1) - t(k-1)} \tag{27}$$

where $t(k+1)$ and $t(k-1)$ denote the sampling times corresponding to the states, observed by a sensor, $x(k+1)$ and $x(k-1)$.

Now we can estimate all the parameters using an unconstrained least squares approach:

$$\widehat{\theta_d} = \arg_\theta \min \frac{1}{K} \sum_{k=1}^{K} [\ \hat{\dot{x}}(k) - \phi(k)^T \theta\ ]^2 \tag{28}$$

where the parameters θ are defined as before, but the measurements ϕ are not restricted to the steady state values, i.e. ϕ includes transient measurements. Then, applying the matrix formulation (see Appendix A) the estimate of the parameters is simply obtained by a pseudo-inverse, taking a particular case of the equation (45):

$$\widehat{\theta_d} = (\phi_K^T \phi_K)^{-1} \phi_K^T d_X \tag{29}$$

where $d_X = [\hat{\dot{x}}(1)\ \hat{\dot{x}}(2)\ \cdots\ \hat{\dot{x}}(K)]^T$.

C. Simulation based Uncertainty Analysis

We have one infrared sensor, composed of one emitter and one receiver, that measure the fan speed in rotations per second, [rps], and we aim to assess the effect on the estimations of the possible lack of precision of the sensor. The reason for this study is owing to a number of parametric fitting experiments that showed there is an upper level of sensor noise above which the parametric fitting methodology breaks down.

Having estimated parameters for a real system approximated by model (21), allows simulating the real system, adding noise to the sensor values, and therefore verify the sensitivity of the estimation process with respect to sensor noise.

To build a simulated model of the real system is used the Simulink tool from Matlab following the equation (21) as it shows the figure 7. As in the real system, the input is a reference voltage and the output, which is equal to the system state, is the propeller rotation speed.

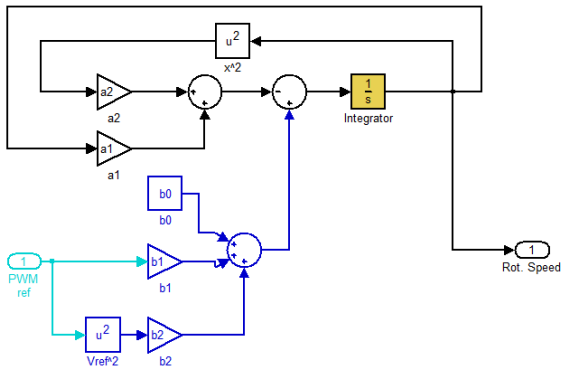

Fig. 7. Power-Motor-Propeller Simulink model used in the experiments.

In order to assess the parametric fitting methodology with the noisy data, is added Gaussian noise to the output of the PMP system. We add Gaussian noise to the output of our Simulink model, using the *Gaussian noise generator* box. See figure 8.

The Simulink model allows simulating our system and obtaining all the required signals, namely input, state and derivative state signals. Given these signals, we compute the value of our parameters as described in (29).

An important simulation aspect to be noted is the setting of *Seeds*, a property of the noise box in Simulink. *Seeds* have been set in order to make the experiments repeatable. Multiple values have been chosen to obtain statistical meaning. The

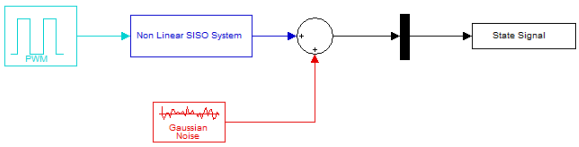

Fig. 8. Power-Motor-Propeller Simulink model with added Gaussian noise in its output. The block named *Non Linear SISO System* is the PMP model, detailed in figure 7.

Seeds used in all our simulations are equal separated by 2122 distance, starting and finishing at 0 and 23343 respectively.

Having in mind reading the error results of our estimations versus a possible error in our sensor, it is more convenient to have a disturbance in the same units of the output of the system. Therefore, we have chosen the standard deviation, $\rho = \sqrt{\sum_{i=1}^{N} \frac{\dot{\theta(i)}^2}{N}}$ as it has [rps] units. The maximum standard deviation was selected such that median fitting errors would be under 50%.

One way to plot fitting errors is using the Root Mean Squared Error (RMS):

$$RMSE = \sqrt{\frac{1}{N}\sum_{i=1}^{N}(\hat{x_i} - x_i)^2} \ . \tag{30}$$

where $\hat{x_i}$ is our fan speed estimator and x_i is the fan speed of the real system.

Alternatively, we can use also an average of relative errors, computed per sample

$$E_{\%} = \frac{1}{N}\sum_{i=1}^{N}\left|\frac{\hat{x}_i - x_i}{x_i}\right| \times 100 \tag{31}$$

since our measurements x_i are in essence positive, not zero, values.

V. Experiments

A. Data Acquisition

The input (PWM) voltage drives a Propeller coupled to a DC motor, through a MOSFET. Figure 9 shows pictures of the system (see also figure 6 for an explaining diagram). The propeller lifts the ball. In this work we model the reference voltage to the propeller rotation speed. In order to obtain rotation speed measurements we use an infra-red LED emitter (see figure 9(b)) and an infra-red receiver (see figure 9(c)). The blades of the propeller interrupt the infra-red path, twice for each complete rotation, and therefore allow observing the rotation speed by counting half the number of interruptions per second (units are therefore rotations per second, rps).

An important aspect to be considered is the possible error on the measurements due to sampling frequency. This parameter is critical to obtain accurate data. In the following we show that in our setup the sampling frequency is enough to cause a lesser than 1% error on rps measurements.

In order to measure speed is necessary to wait the two blades to pass in front of the IR sensor and cut the light of the

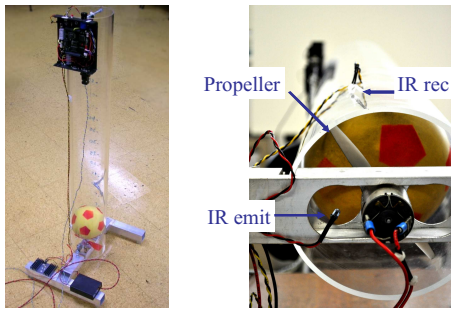

(a) Setup (b) Bottom view

Fig. 9. Detailed view of the setup. The bottom view focus the IR emitter and the motor (b).

IR emitter. Considering the highest speed of the motor to be $x = 200$ rps, one has the maximum of 400 pulses per second observed in the IR sensor. In other words, one has a time of $t_p = 1/400\ sec$ between blades and $x = 1/(2t_p)$.

All the measurements from the real system were taken by a data acquisition board from National Instruments. This board is able to acquire 100000 samples per second, i.e. allows a sampling period of $T_s = 10\ \mu sec$. Assuming a $\pm T_s$ error in the beginning and the ending of measuring t_p, one has the maximum error of $e_x = 2T_s/(t_p - 2T_s) \approx 0.8\%$.

B. System Identification

In this section we identify our system by estimating the parameters of the proposed model. To obtain these parameters we test the system with different steps. In our case we have created two datasets encompassing (i) three or (ii) ten step responses within the range of the PWM input signal. In addition to the step responses we compute also their derivative using a first order difference.

In this section we consider two different ways to represent our system. In the first representation we have parameters a_1, a_2, b_0 and b_1 hence giving more importance to non linearity on the output side (Fan):

$$\dot{x} + a_1 x + a_2 x^2 = b_0 + b_1 u \tag{32}$$

In the second representation we assume $a_2 = 0$ and $b_2 \neq 0$ hence giving relevance to the input side or Power Driver

$$\dot{x} + a_1 x = b_0 + b_1 u + b_2 u^2 \tag{33}$$

1) Three Step Responses Dataset: As it could be seen in figure 10 in the first place starting for the top we have the input values, in the middle we observe the state information or speed rotation of the blades and derivative state in the last place. The parameter results obtained applying the methodology are in the table I.

The parameter results obtained applying the methodology are in the table I.

Given the estimated Power-Motor-propeller system parameters allows building a Matlab/Simulink model and simulating step responses. This model follows the same form of the equation (21). See figure 7 . Figure 11 shows the identification results given the three steps dataset.

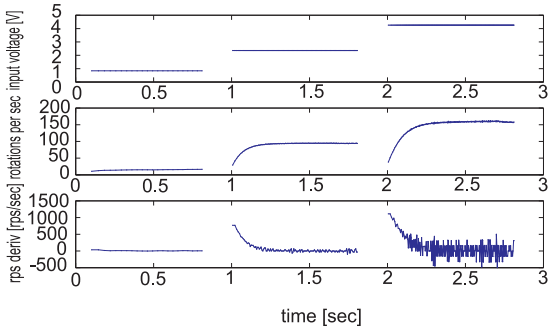

Fig. 10. Dataset encompassing 3 step responses. PWM step signals (top), rotation speed (middle) and numerical derivative of the rotation speed (bottom).

Exp.	a_1	a_2	b_0	b_1	b_2	$RMSE$ [rps]	$E_{\%}$ (eq.(31))
1	4.86	0.027	-209.65	391.42	–	4.21	17.77 %
2	11.16	–	-442.5	787.42	-62.48	2.17	4.71 %

TABLE I
PARAMETERS AND FITTING ERROR ESTIMATED FROM THE THREE STEPS DATASET.

2) Ten Step Responses Dataset: In this section are shown the results of our estimator with 10 different input steps from 0 to 5 Volts.

The figure 12 show us an increasing inaccuracy on the speed and acceleration of the blades when the input steps grow. This fact has different interpretations that will be commented in the conclusion section. The parameter estimation results obtained can be watched in table II.

Exp.	a_1	a_2	b_0	b_1	b_2	$RMSE$ [rps]	$E_{\%}$ (eq.(31))
1	4.89	0.03	-274.94	436.02	–	3.9	15.23 %
2	11.62	–	-478.11	828.57	-65.87	1.72	2.96 %

TABLE II
ESTIMATED PARAMETERS FOR THE 10 STEPS DATASET.

In figure 13(a) we use the parameters listed in the second row of the table II that is the equation (33). Taking the other

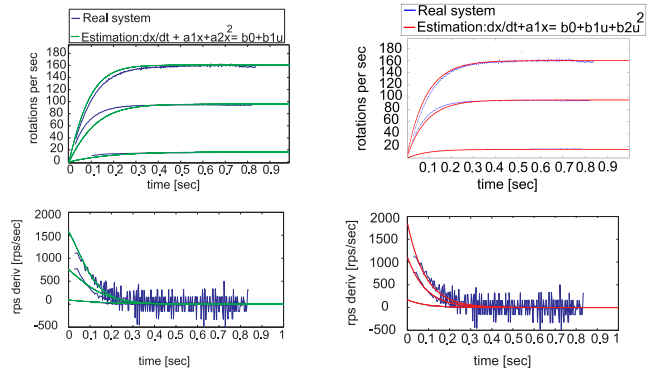

(a) Model of eq. (32) (b) Model of eq. (33)

Fig. 11. Real system vs simulated system, rotation speed step responses (top) and rotation acceleration (bottom). Comparing $(a_2 \neq 0, b_2 = 0)$ with $(a_2 = 0, b_2 \neq 0)$, left vs right column, respectively.

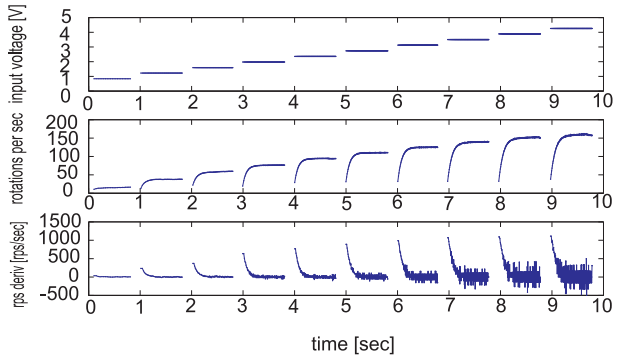

Fig. 12. Dataset encompassing 10 step responses.

non linear system parameters, first row of the table II that is the equation (32) allows obtaining 13(b).

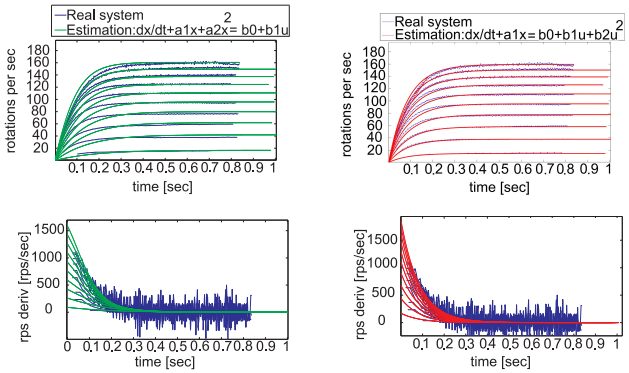

(a) Model of eq. (32) (b) Model of eq. (33)

Fig. 13. Real system vs simulated system, rotation speed step responses (top) and rotation acceleration (bottom). Comparing $(a_2 \neq 0, b_2 = 0)$ with $(a_2 = 0, b_2 \neq 0)$, left vs right column, respectively.

The results and pictures showed during this section provide information about the differences between both system models and the accuracy in relation to the real system.

Results show that model (33) has a dynamics and steady state closer to the real system than model (32).

The fitting error reasserts this fact with the data provided in the table II and I with a significant difference between both models in terms of the RMSE and fitting error results, more than 2 rps and 10% fitting error. Is important to watch that 10 step responses, table II provide a little bit more accuracy than the table I. For that reason is chosen the model (33) 10 step responses data to do the next experiments.

C. Noise Analysis

In this section we assess the system identification methodology under the effect of noise in the sensed data. More in detail, we use the parameters estimated in the last section to simulate the non-linear system. The simulated system is then used to estimate again the system parameters, given step responses of the system containing additive Gaussian noise. The global Simulink model is shown in figure 8, while the detailed power-motor-propeller system is the one shown in Fig.7.

The box plot representation give us a way to observe an amount of different data, as the mean, the dispersion and symmetry of all the data obtained in the simulations.

The results shown in figure 14 are generated with the aim to visualize the error in our estimations until a 50% upper bound. We have chosen a noise limit of 6 rps.

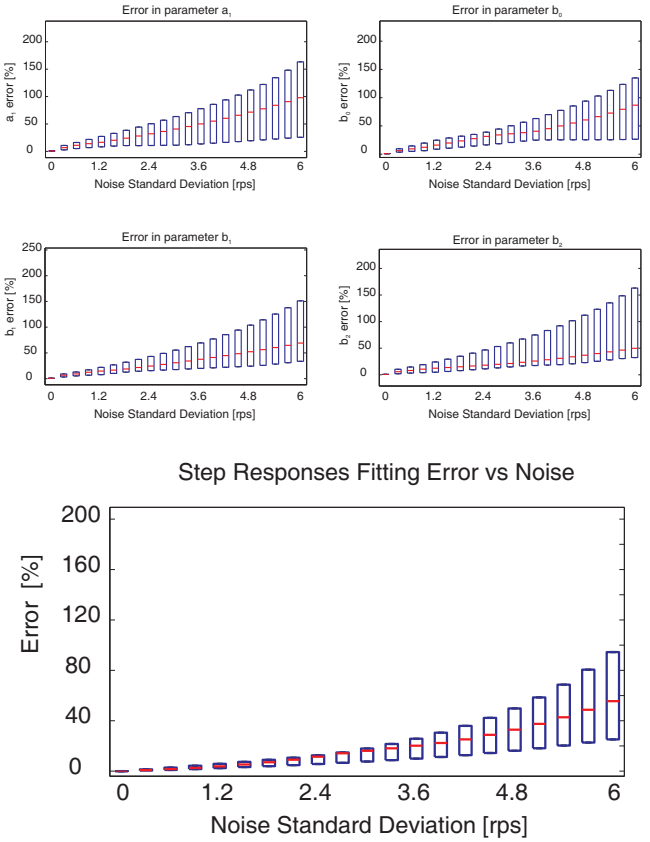

Fig. 14. Fitting error given Gaussian noise with various standard deviations (maximum 6 rps). Error in parameters a_1, b_0, b_1, b_2, and error in the step response.

A first observation is the relationship between the parameters and the response. More sensor noise implies more fitting error. In another hand the results show a lower fitting error for a higher index i in b_i. For example an error b_2 has a 50% fitting error instead of almost 100% of the parameter b_0.

The box-plot representation is used to watch easily the data dispersion. The box-plot provides us the following information: (i) the data dispersion becomes higher with an increasing noise, this feature could be seen with the box height, higher means more dispersion, (ii) in the most cases the dispersion is symmetric as in the highest and in the lowest values and this it could be seen with the position of the mean red line inside the box.

VI. Conclusion and Future Work

In this work has been proposed a parametric model and a method to identify the parameters of the power-driver, DC-motor and propeller non-linear system.

Two main aspects have been studied in this work: (i) identification of the most relevant non-linear model components, (ii) the effect of the sensor error, i.e. the error in the rotations per second measurements, in the accuracy of the fitted model.

The identification section shows the difference of considering the non-linearity of the power driver vs the non-linearity introduced by the propeller. Both system models are tested with the same data. In our case the dynamics of Power Driver (MOSFET) are more relevant than the propeller, most probably due to the fact that it is lifting just a very-light-weighted ball. However if the propeller would be working in different conditions, e.g. within denser fluids as water, or higher pressures, this fact could change.

The decision of choosing a sensor is critical to the estimation. This is the second main conclusion of this thesis. Just a small error counting the passes of the blades of the propeller has a dramatic impact on the accuracy provided by the least squares estimation. For example, a bad measurement of 6 rps on the 200 rps rotation speed introduces a 60% error on the estimation.

As future work, it would be interesting to research more the nature of sensor noise and improve the estimation methodologies so that the sampling frequency can be minimized.

Additionally, as a future work it is our goal to include the levitating ball pressure and gravity based dynamics, i.e. modeling the complete dynamic process from the reference PWM signals to the ball levitating height.

Appendix

In [2, page 463], Ljung introduces a parametric model identification methodology based in least squares. The objective of the methodology is to find the most accurate prediction (fitting) of a system output time function, *y(t)*, given measurements of variables, $\phi_1(t), ..., \phi_d(t)$, which are combined to form the output time function:

$$y(t) = \theta_1\phi_1(t) + \theta_2\phi_2(t) + ... + \theta_N\phi_N(t). \tag{34}$$

Defining the parameters vector

$$\theta = [\theta_1\theta_2...\theta_N]^T \tag{35}$$

and the measurements matrix

$$\phi(t) = [\phi_1(t)\ \phi_2(t)\ \cdots\ \phi_N(t)] \tag{36}$$

where t takes values in a finite set, one has the system model:

$$y(t) = \phi^T(t)\theta. \tag{37}$$

In summary, considering N time samples, one has the data set:

$$\{(y(t), \phi(t)) : \quad t = 1, ..., N\}. \tag{38}$$

and the objective is to estimate the vector of parameters θ. In order to estimate θ one may minimize the variance Denoting variance as:

$$V_N(\theta) = \frac{1}{N}\sum_{t=1}^{N}[y(t) - \phi^T(t)\theta]^2 \tag{39}$$

the minimization problem can be stated as:

$$\widehat{\theta_N} = arg_\theta \min \frac{1}{N}\sum_{t=1}^{N}[y(t) - \phi^T(t)\theta]^2. \tag{40}$$

Equation (40) can be minimized analytically and expressed all the $\widehat{\theta_N}$ that satisfies the minimum of $V_N(\theta)$ as the normal equations notation as follows:

$$\widehat{\theta_N} = [\frac{1}{N}\sum_{t=1}^{N}\phi(t)\phi^T(t)]^{-1}\frac{1}{N}\sum_{t=1}^{N}\phi(t)y(t) \tag{41}$$

The equation (40) shows the best accurate estimator to get the system parameters.

A solution can also be obtained using matrix notation. Considering N time samples, equations (38) to (40) can be rewritten as:

$$Y_N = \begin{bmatrix} y(1) \\ y(2) \\ \vdots \\ y(N) \end{bmatrix} \text{ and } \phi_N = \begin{bmatrix} \phi^T(1) \\ \phi^T(2) \\ \vdots \\ \phi^T(N) \end{bmatrix}$$

where Y_N is a $N \times 1$ column vector and ϕ_N is a $N \times d$ matrix. The matrix ϕ_N is composed by the $1 \times d$ vector

$$\phi(N) = [x(N)\ x(N)^2\ ...\ x(N)^d], \tag{42}$$

where d the number of parameters chosen to represent the system, and $x(N)$ is the measured variable at time N. Then, equation (39) can be written with the matrix formulation as follows:

$$V_N(\theta) = \frac{1}{N}\left|Y_N - \phi_N\theta\right|^2 = \frac{1}{N}(Y_N - \phi_N\theta)^T(Y_N - \phi_N\theta) \tag{43}$$

In this notation the normal equations taking the equation (41) are :

$$[\phi_N^T\phi_N]\widehat{\theta_N} = \phi_N^T Y_N \tag{44}$$

and the estimate take the following form

$$\widehat{\theta_N} = \theta_N^+ Y_N \tag{45}$$

where

$$\theta_N^+ = [\phi_N^T\phi_N]^{-1}\phi_N^T \tag{46}$$

As it could be seen the equation (46) is the pseudo inverse of $\widehat{\theta_N}$.

REFERENCES

[1] Michel Fliess, Cédric Join, and Herbertt Sira-Ramírez. Non-linear estimation is easy. *Int. Journal of Modeling, Identification and Control*, 3, 2008.

[2] Lennart Ljung. *System identification. Theory for the user*. Prentice-Hall, inc., 1991.

[3] Marcos Pascual Moltó, Emilio Figueres Amorós, Diego Cerver Lloret, José Manuel Benavent Garcia, and Gabriel Garcerà Sanfeliu. *Componentes Electrónicos de Potencia. Características, protecciones y circuitos de disparo*. Universitat Politècnica de València.

[4] E. Morgado, F. M. Garcia, J. Gaspar, and Ana Fred. *Controlo digital de velocidade de um motor D.C. (in Portuguese)*. University of Lisbon, Portugal, 2013.

[5] Carlos Silvestre. *Manual for the Final Project of the course Distributed Real Time Control Systems (in Portuguese)*. Technical University of Lisbon, Portugal, 2005.

[6] Josef Zehetner, Johann Reger, and Martin Horn. A derivative estimation toolbox based on algebraic methods - theory and practice. In *IEEE Int. Conf. on Control Applications*, 2007.